J|A|C|S
ARTICLES
Published on Web 06/14/2006

# High Triplet Energy Polymer as Host for Electrophosphorescence with High Efficiency

Yen-Chun Chen, Guo-Sheng Huang,† Chung-Chin Hsiao, and Show-An Chen*

*Contribution from the Chemical Engineering Department, National Tsing-Hua University, Hsinchu, 30041, Taiwan, R.O.C.*

Received February 8, 2006; Revised Manuscript Received April 3, 2006; E-mail: sachen@che.nthu.edu.tw

***Abstract:*** We report the conjugated polymer P(*t*Bu-CBP) as a host with high triplet energy ($E_T$ 2.53 eV) and suitable HOMO (5.3 eV) and LUMO (2.04 eV) energy levels. Upon doping with green and red emission Ir-complexes, it gives devices with high luminous and external quantum efficiencies for green emission (23.7 cd/A, 6.57%) and for red emission (5.1 cd/A, 4.23%), respectively, and low turn-on voltage (3 V). For both devices, the efficiencies are higher than those of the corresponding devices with the same backbone P(3,6-Cz) as a host by a factor of 4, even though the latter has an $E_T$ (2.6 eV) slightly higher than that of the former. The results reflect that, in phosphorescent devices, the difference in $E_T$ between the host and guest is not the only factor that determines the device efficiency, and the present side group modification via the 9 position of carbazole also plays an important role, which allows a tuning of HOMO and LUMO levels to provide more balance in electron and hole fluxes and provides prevention from formation of excimer.

## Introduction

Doping heavy metal complexes[1] (e.g., Ir and Pt complexes) into host materials in an organic light emitting diode for obtaining high external quantum efficiency has attracted great attention, owing to their efficient intersystem crossing from singlet to triplet excited states followed by relaxing through phosphorescence. Thus, an electrophosphorescent (EP) device, allowing us to harvest both singlet and triplet excitons, is an efficient approach over a purely fluorescent device where only singlet exciton provides a radiative pathway. For an efficient device, the host matrix should fulfill energy-level matching with neighboring layers or electrodes for efficient charge injections and with the guest for effective energy transfer of singlet excitons and for efficient triplet confinement at the guest[2] (requiring a higher triplet energy $E_T$ than that of the guest). Studies on a high efficiency EP device with a conjugated polymer as a host in red emission have been extensive,[3] but in green[4a] and blue emissions they are scarce due to the unavailability of high $E_T$ polymers (at least higher than the $E_T$ of the green guest 2.4 eV for an Ir-complex).[2b] Recently a polycarbazole (P(3,6-Cz)) with an interconnection of carbazole units in 3,6 positions was reported as a potential candidate for a host from a quantum-chemical study[4b−4c] and found experimentally[4a] to give a high efficiency green device (16 cd/A) when doped with a green emitting Ir-complex. This polymer possesses high $E_T$ (2.6 eV) and suitable highest occupied molecular orbital (HOMO, 5.25 eV) and lowest unoccupied molecular orbital (LUMO, 2.05 eV) levels allowing ease of charge injections relative to the anode poly-(3,4-ethylenedioxythiophene):poly-(styrenesulfonate) (denoted as PEDOT:PSS for simplicity) and cathode (Ba/Al). However, it has drawbacks: imbalanced charge fluxes[4a] and formation of a lower energy emission band, which was claimed as an excimer emission.[5] The formation of excimer usually lowers the photoluminescence quantum efficiency (PLQE) resulting in a lowering rate constant for the Förster energy transfer.[6]

† Present address: National Laboratory of Applied Organic Chemistry, Lanzhou University, Lanzhou 730000, China.

(1) (a) Baldo, M. A.; O'Brien, D. F.; Shoustikov, A.; Sibley, S.; Thompson, M. E.; Forrest, S. R. *Nature* **1998**, *395*, 151−154. (b) Baldo, M. A.; Thompson, M. E.; Forrest, S. R. *Nature* **2000**, *403*, 750−753. (c) Lamansky, S.; Djurovich, P. I.; Murphy, D.; Abdel-Razzaq, F.; Kwong, R.; Tsyba, I.; Bortz, M.; Mui, B.; Bau, R.; Thompson, M. E. *Inorg. Chem.* **2001**, *40*, 1704−1711. (d) Lamansky, S.; Djurovich, P.; Murphy, D.; Abdel-Razzaq, F.; Lee, H.-E.; Adachi, C.; Burrows, P. E.; Forrest, S. R.; Thompson, M. E. *J. Am. Chem. Soc.* **2001**, *123*, 4303−4312.

(2) (a) Sudhakar, M.; Djurovich, P. I.; Hogen-Esch, T. E.; Thompson, M. E. *J. Am. Chem. Soc.* **2003**, *125*, 7796−7797. (b) Chen F.-C.; He, G.; Yang, Y. *Appl. Phys. Lett.* **2003**, *82*, 1006−1008. (c) Adachi, C.; Kwong, R. C.; Djurovich, P.; Adamovich, V.; Baldo, M. A.; Thompson, M. E.; Forrest, S. R. *Appl. Phys. Lett.* **2001**, *79*, 2082−2084. (d) Holmes, R. J.; Forrest, S. R.; Tung, Y.-J.; Kwong, R. C.; Brown, J. J.; Garon, S.; Thompson, M. E. *Appl. Phys. Lett.* **2003**, *82*, 2422−2424. (e) Tokito, S.; Iijima, T.; Suzuri, Y.; Kita, H.; Tsuzuki, T.; Sato, F. *Appl. Phys. Lett.* **2003**, *83*, 569−571. (f) Holmes, R. J.; D'Andrade, B. W.; Forrest, S. R.; Ren, X.; Li, J.; Thompson, M. E. *Appl. Phys. Lett.* **2003**, *83*, 3818−3820.

(3) (a) Chen, X.; Liao, J. L.; Liang, Y.; Ahmed, M. O.; Tseng, H. E.; Chen, S. A. *J. Am. Chem. Soc.* **2003**, *125*, 636−637. (b) Jiang, C.; Yang, W.; Peng, J.; Xiao, S.; Cao, Y. *Adv. Mater.* **2004**, *16*, 537−541. (c) Wu, F. I.; Shih, P. I.; Tseng, Y. H.; Chen, G. Y.; Chien, C. H.; Shu, C. F.; Tung, Y. L.; Chi, Y.; Jen, A. K. Y. *J Phys. Chem. B* **2005**, *109*, 14000−14005. (d) Gong, X.; Ostrowski, J. C.; Bazan, G. C.; Moses, D.; Heeger, A. J.; Liu, M. S.; Jen, A. K. *Adv. Mater.* **2003**, *15*, 45−49. (e) Sandee, A. J.; Williams, C. K.; Evans, N.; Davies, J. E.; Boothby, C. E.; Kohler, A.; Friend, R. H.; Holmes, A. B. *J. Am. Chem. Soc.* **2004**, *126*, 7041−7048. (f) Jiang, J.; Jiang, C.; Yang, W.; Zhen, H.; Huang, F.; Cao, Y. *Macromolecules* **2005**, *38*, 4072−4080. (g) Zhen, H.; Luo, C.; Yang, W.; Song, W.; Du, B.; Jiang, J.; Jiang, C.; Zhang, Y.; Cao, Y. *Macromolecules* **2006**, *39*, 1693−1700.

(4) (a) Dijken, A. v.; Bastiaansen, J. J. A. M.; Kiggen, N. M. M.; Langeveld, B. M. W.; Rothe, C.; Monkman, A. P.; Bach, I.; Stössel, P.; Brunner, K. *J. Am. Chem. Soc.* **2004**, *126*, 7718−7727. (b) Marsal, P.; Avilov, I.; da Silva Filho, D. A.; Brédas, J. L.; Beljonne, D. *Chem. Phys. Lett.* **2004**, *392*, 521−528. (c) Avilov, I.; Marsal, P.; Brédas, J. L.; Beljonne, D. *Adv. Mater.* **2004**, *16*, 1624−1629.

(5) (a) Siove, A.; Adès, D. *Polymer* **2004**, *45*, 4045−4049. (b) Zhang, Z. B.; Fujiki, M.; Tang, H. Z.; Motonaga, M.; Torimitsu, K. *Macromolecules* **2002**, *35*, 1988−1990.

(6) Förster, T. *Discuss. Faraday Soc.* **1957**, *27*, 7−17.

***Scheme 1.*** Synthetic Route for Intermediate **5**

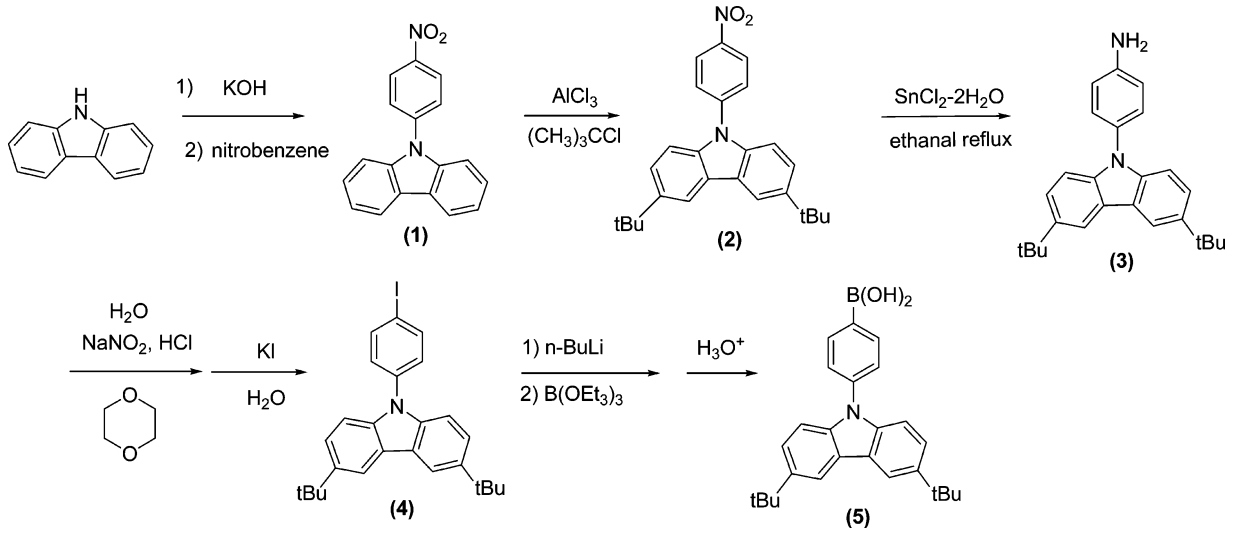


***Scheme 2.*** Synthetic Route for Intermediates **7** and **8**

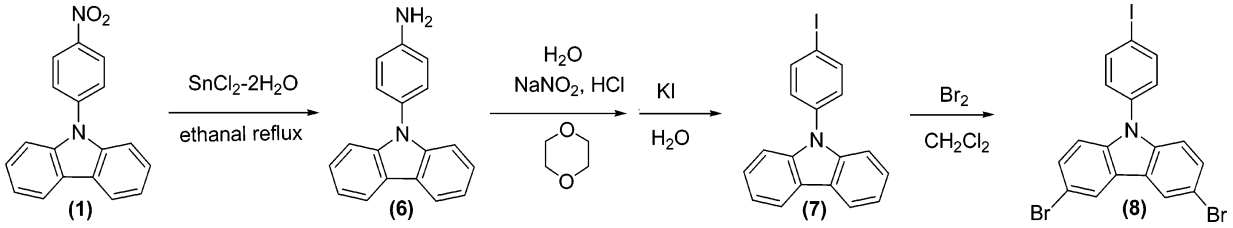


***Scheme 3.*** Synthetic Route for Monomer **9** and Compound **10**

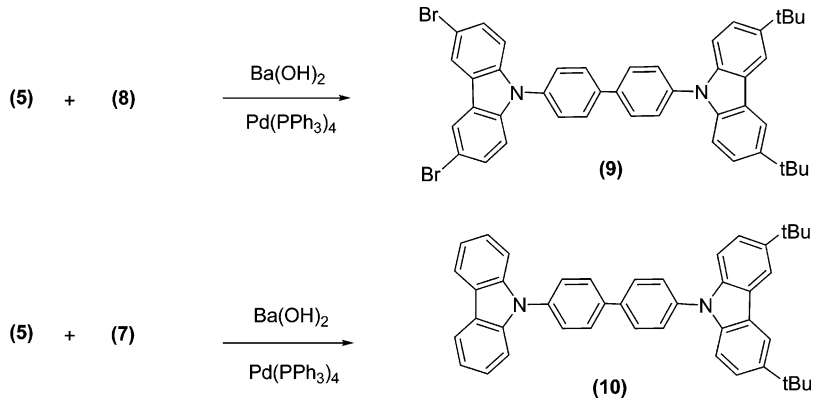


Here, we report the conjugated polymer P(*t*Bu-CBP) (Scheme 4) for use as a host which possesses high $E_T$ (2.53 eV) and suitable HOMO (5.3 eV) and LUMO (2.04 eV) energy levels. Upon doping with green and red emission Ir-complexes, it gives devices with high luminous and external quantum efficiencies for green emission ($\eta_{Lmax} = 23.7$ cd/A, $Q_{ext} = 6.57\%$) and for red emission ($\eta_{Lmax} = 5.1$ cd/A, $Q_{ext} = 4.23\%$), respectively, and low turn-on voltage (3 V). For both devices, the efficiencies are higher than those of the corresponding devices with P(3,6-Cz) as the host by a factor of 4, even though the latter has an $E_T$ (2.6 eV) slightly higher than that of the former. Evidently, the device efficiency of the phosphorescent emission is not solely dependent on the difference in $E_T$ between the host and guest, and the side group in P(*t*Bu-CBP) also plays an important role. Incorporations of the comonomers with higher $E_T$ values, dialkoxy substituted phenylene (compound **12**) and dialkyl substituted fluorene (compound **11**), on the main chain to give the alternating copolymers P(*t*Bu-CBP*P*) and P(*t*Bu-CBP*F*) (Scheme 5), do not promote, in fact decrease, the levels of $E_T$ and therefore lower the device efficiency due to back energy transfer of $E_T$.

## Experimental Section

**Synthesis of Monomers and Polymers.** The synthetic routes for the intermediates of monomers, monomers, and polymers used are described in Schemes 1−5. The preparations of polymers P(3,6-Cz) and P(*t*Bu-CBP) were conducted using the Yamamoto coupling reaction. P(*t*Bu-CBP*P*) and P(*t*Bu-CBP*F*) were prepared by the Suzuki coupling reaction. The detailed synthetic procedures for the monomers and polymers are described in the Supporting Information (SI).

**Instrumentation.** Ultraviolet−visible (UV−vis), photoluminescence (PL), photoexcitation (PLE), electroluminescence (EL), phosphorescence, ultraviolet photoemission spectra (UPS), scanning probe microscopy, gel permeation chromatography (GPC), scanning probe

***Scheme 4.*** Synthetic Route for the Polymers P(*t*Bu-CBP) and P(3,6-Cz)

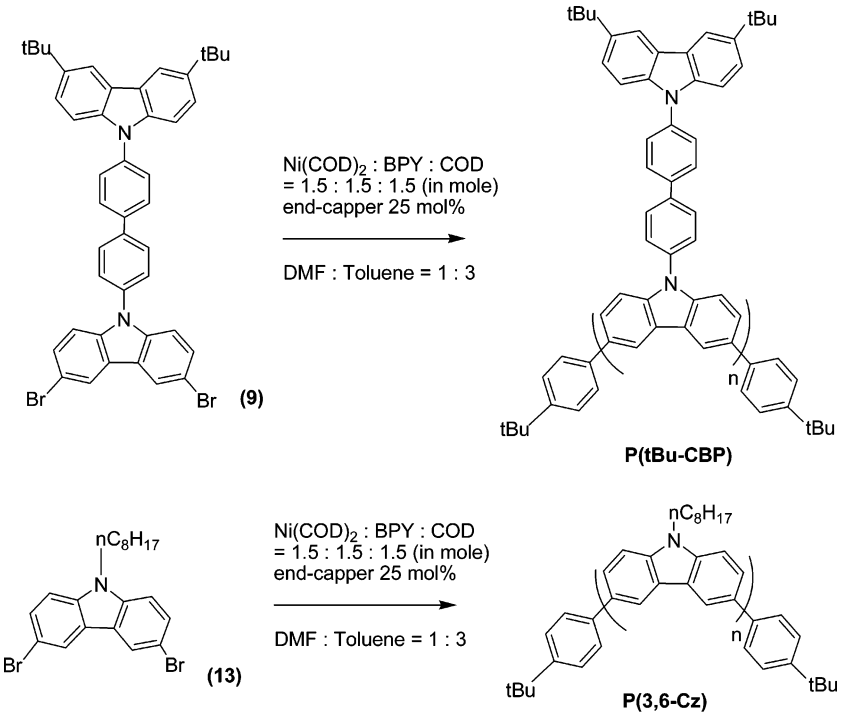


***Scheme 5.*** Synthetic Route for the Copolymers P(*t*Bu-CBP*F*) and P(*t*Bu-CBP*P*)

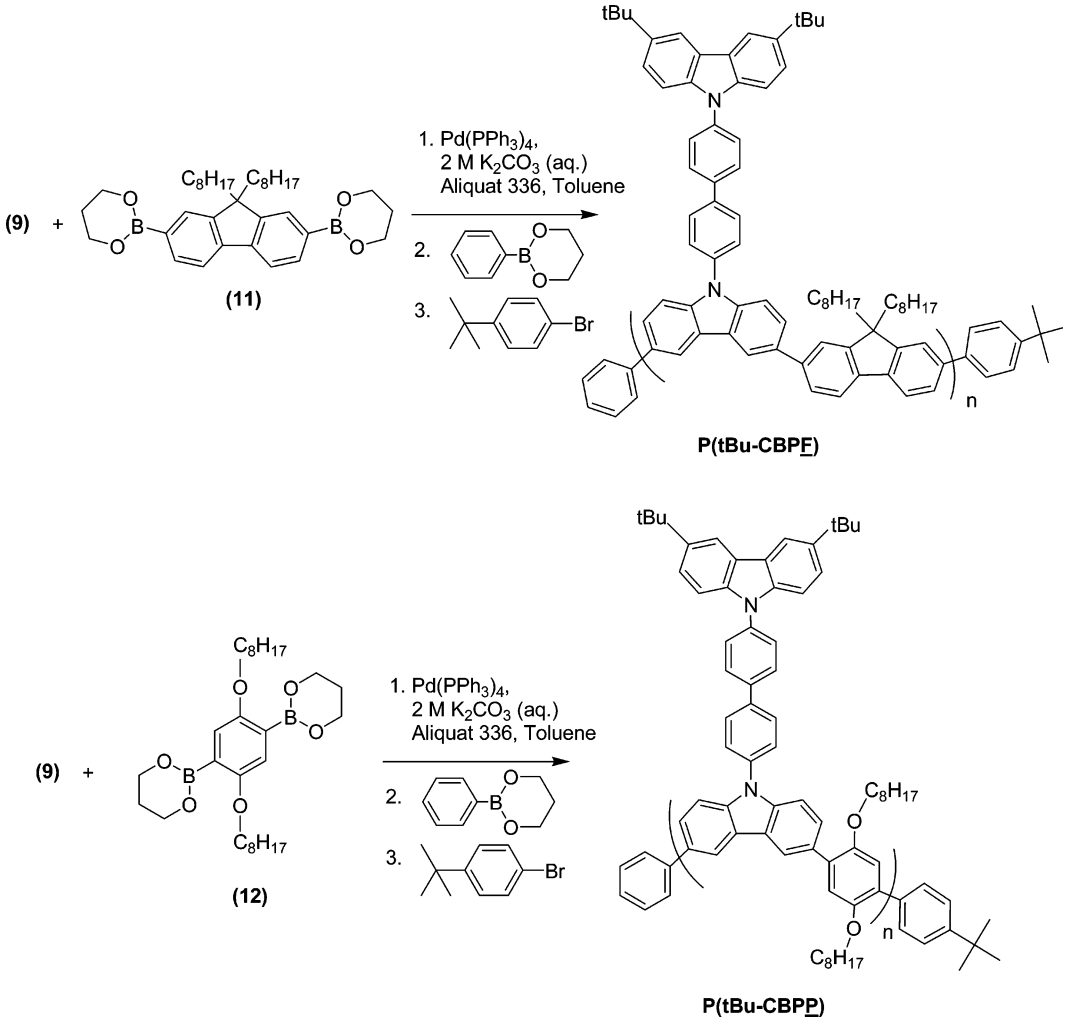

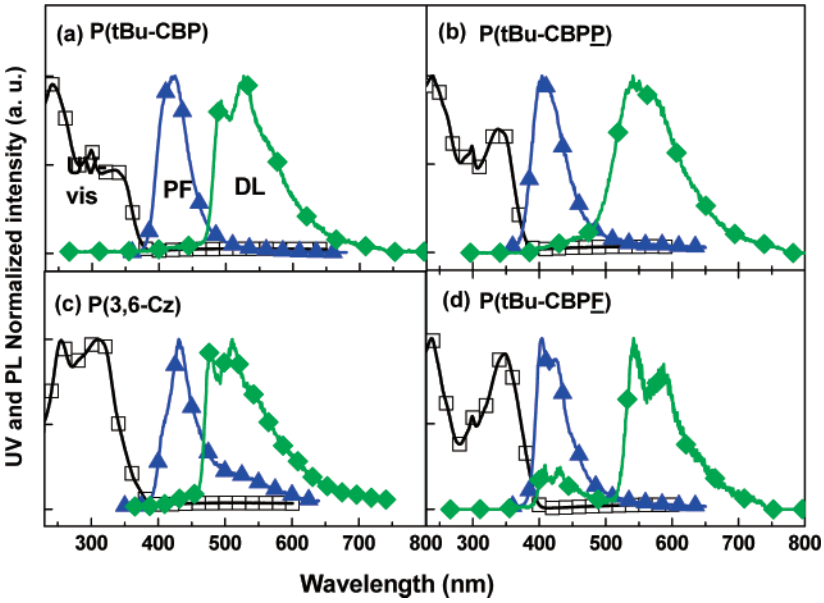


***Figure 1.*** UV−vis (□) and prompt fluorescence (PF) (▲) at room temperature, and delay luminescent (DL) with delay time of 5 ms after photoexcitation (◆) spectra at 4 K of P(*t*Bu-CBP), P(3,6-Cz), P(*t*Bu-CBP*P*), and P(*t*Bu-CBP*F*) thin solid films.

microscopy (SPM), film thickness monitor and power supplies and luminance meter for measurements of device performance are also described in detail in the SI.

**Device Fabrication and Characterization.** An indium−tin oxide (ITO) glass was exposed on oxygen plasma at a power of 50 W and a pressure of 200 mTorr for 5 min. A thin layer (15 nm) of poly(styrene sulfonic acid)-doped poly(ethylenedioxythiophene) (Baytron P CH 8000 from Bayer, its conductivity is $10^{-5}$ S/cm) was spin-coated on the treated ITO as a hole injection layer. Polymer solutions of P(3,6-Cz) and P(*t*Bu-CBP) in chlorobenzene (20 mg/mL) were filtered through a 5 $\mu$m filter and then spin-coated on top of the PEDOT:PSS layer. The 1,3,5-tris(2-henylbenzimidazolyl)benzene (TPBI) layer (30 nm), which was used as a hole/exciton blocking layer,[7] was grown by thermal evaporation in a vacuum of $2 \times 10^{-6}$ Torr. Finally, a thin layer of CsF (about 2 nm) covered with a layer of aluminum for a bipolar device was deposited in a vacuum thermal evaporator through a shadow mask at a vacuum of $2 \times 10^{-6}$ Torr. The active area of the device was about 10 mm$^2$. The bipolar device structure was ITO/PEDOT:PSS (15 nm)/Polymer or doped polymer (80 nm)/TPBI (30 nm)/CsF (2 nm)/Al. The fabrication of a single carrier device was similar to that of the bipolar device, but the device structures were different. The structure of the hole dominating device was ITO/PEDOT:PSS (15 nm)/Polymer (120 nm)/Au and that of the electron dominating device was ITO/Ca (50 nm)/polymer (120 nm)/Ca (3 nm)/Al.

## Results and Discussion

**A. Energy Levels Determinations (Singlet, Triplet, HOMO, and LUMO).** The chemical structures for the CBP-based polymers, P(*t*Bu-CBP), P(*t*Bu-CBP*P*) and P(*t*Bu-CBP*F*), and P(3,6-Cz) are shown in Schemes 4 and 5, and their optical spectra (UV−vis, prompt fluorescence (PF), and delay luminescence (DL) spectra) are shown in Figure 1. The homopolymer P(*t*Bu-CBP) exhibits absorption peaks at 238, 300, and 334 nm, which are similar to those of its repeat unit resemblance (*t*Bu-CBP) and monomer (*t*Bu-CBP-Br) (Figure S2) (whose chemical structures are referred to compounds **10** and **9** in Scheme 3, respectively), but its absorption onset shows a red shift by 16 nm as compared to the latter's due to a delocalization of $\pi$-electrons along the polymer backbone. For the absorption spectra of the alternating copolymers, P(*t*Bu-CBP*P*) and P(*t*Bu-CBP*F*), the two higher energy peaks remain unchanged but the lower energy peaks at 337 and 344 nm show red shifts by 3 and 9 nm, respectively, as compared to that of P(*t*Bu-CBP). For P(3,6-Cz), it shows a totally different shape of absorption spectrum as compared to the CBP-based polymers; its absorption peaks at 255 and 320 nm are the same as those with difference alkyl substituents[4a,5b,8] and similar to the characteristic absorption peaks of carbazole dimer rather than those of a carbazole monomer.[8a,c−d]

***Table 1.*** Triplet Energy, HOMO and LUMO Levels, PLQE, and Hole Injection Barrier of the Polymers

| polymer | $E_T$ (eV) | HOMO (eV) | LUMO (eV) | PLQE (%) | hole injection barrier[a] (eV) |
|---|---|---|---|---|---|
| P(*t*Bu-CBP) | 2.53 | 5.3 | 2.0 | 20 | 0.3 |
| P(*t*Bu-CBP*P*) | 2.3 | 5.4 | 2.2 | 64 | 0.4 |
| P(*t*Bu-CBP*F*) | 2.28 | 5.3 | 2.2 | 81 | 0.3 |
| P(3,6-Cz) | 2.6 | 5.0 | 1.8 | 3 | 0.0 |

[a] The difference in HOMO levels between the polymer and PEDOT:PSS (5.0 eV), which are measured by ultraviolet photoelectron spectroscopy.

The emission peaks (PF in Figure 1) are observed at 416 nm with a shoulder at 400 nm for P(*t*Bu-CBP) and at 430 nm with a shoulder at 400 nm and a low-energy band centered at about 525 nm for P(3,6-Cz). P(*t*Bu-CBP*P*) exhibits a peak maximum at 403 nm, and P(*t*Bu-CBP*F*) exhibits maxima at 403 and 423 nm with a shoulder at 450 nm. The corresponding PLQE of those polymers are shown in Table 1 and that of P(*t*Bu-CBP) (20%) is higher than that of P(3,6-Cz) (3%) due to the absence of excimer emission[5] in the former as evidenced by the lack of

(7) Adamovich, V. I.; Cordero, S. R.; Djurovich, P. I.; Tamayo, A.; Thompson, M. E.; D'Andrade, B. W.; Forrest, S. R. *Org. Electron.* **2003**, *4*, 77−87.

(8) (a) Romero, D. B.; Schaer, M.; Leclerc, M.; Ades, D.; Siove, A.; Zuppiroli, L. *Synth. Met.* **1996**, *80*, 271−277. (b) Huang, J.; Niu, Y.; Yang, W.; Mo, Y.; Yuan, M.; Cao, Y. *Macromolecules* **2002**, *35*, 6080−6082. (c) Paliulis, O.; Ostrauskaite, J.; Gaidelis, V.; Jankauskas, V.; Strohriegl, P. *Macromol. Chem. Phys.* **2003**, *204*, 1706−1712. (d) Ostrauskaite, J.; Strohriegl, P. *Macromol. Chem. Phys.* **2003**, *204*, 1713−1718. (e) Iraqi, A.; Wataru, I. *J. Polym. Sci., Part A: Polym. Chem.* **2004**, *42*, 6041−6051.

lower-energy emission band (~525 nm) as to be discussed later in this section. Both the alternating copolymers, P(*t*Bu-CBP*P*) and P(*t*Bu-CBP*F*), have a significant enhancement in PLQE of 64 and 81%, respectively. The delay luminescence (DL) (or phosphorescence) at 4 K as shown in Figure 1 is utilized to determine the $E_T$ of the polymers, in which the first vibronic transition ($T_1^{\nu=0} \rightarrow S_0^{\nu=0}$) of the phosphorescence is assigned as $E_T$.[4a] The $E_T$ of P(*t*Bu-CBP) (2.53 eV, 490 nm) is only slightly lower than that of P(3,6-Cz) (2.6 eV, 478 nm) due to the side group modification. However, upon incorporation of the comonomers, dialkyl substituted fluorene (compound **11**) and dialkoxy substituted phenylene (compound **12**), to yield the copolymers, P(*t*Bu-CBP*F*) and P(*t*Bu-CBP*P*), the $E_T$'s drop significantly to 2.28 eV (545 nm) and 2.3 eV (540 nm), respectively (Figure 1 and Table 1).

The HOMO levels of the polymers are determined from the cyclic voltammetry measurements (experimental detail and results are given in SI section 3) and listed in Table 1; no reduction waves were observed down to about −1.2 V, and all polymers showed irreversible oxidative behavior. The energy level of LUMO was deduced from the onset of the UV−vis spectrum and HOMO level (Table 1). The HOMO level of P(*t*Bu-CBP) 5.3 eV is lower than that of P(3,6-Cz) (5.0 eV). However, the HOMO levels of P(*t*Bu-CBP*P*) (5.4 eV) and P(*t*Bu-CBP*F*) (5.3 eV) are close to that of P(*t*Bu-CBP). The resulting hole injection barriers for these CBP- and Cz-based polymers at the interfaces with PEDOT:PSS are significantly improved relative to those of the mostly investigated polymer hosts PFOs/PEDOT:PSS (0.6−0.8 eV)[2b,3a−c] and PVKs/PEDOT:PSS (~1 eV)[9] and thus can lead to low operating voltage and high device power efficiency.

**B. Variations in Energy Levels of Singlet/Triplet and HOMO/LUMO with Molecular Structures.** The conjugation lengths of carbazole derivatives[4a,10] coupling via its 3,6 positions have been investigated based on the studies for oligophenylenes,[11] in which the $\pi$-electron delocalizations are extended along the longest molecular axis for *para*-linkage with $E_T$ decreasing with the number of phenyls and interrupted at the meta-linkage. For example, the $E_T$ of biphenyl (2.84 eV) is higher than that of *p*-terphenyl (2.55 eV), and the $E_T$ of *m*-terphenyl (2.81 eV) is close to that of biphenyl because its conjugation is interrupted on the meta position for which the triplet state is localized at every composing biphenyl structure.[11] In this respect, Brunner et al.[10a] found that the $E_T$ of a carbazole dimer, linked via the 3,6 position, reduces from a monomer 3.05 eV to a dimer 2.75 eV and is close to that of biphenyl 2.84 eV. This indicates not only that in a carbazole dimer the triplet exciton is more delocalized in the carbazole dimer than in the carbazole monomer but also that the triplet exciton is predominantly delocalized over the biphenyl structure across the neighboring carbazole unit (as illustrated in Figure 2a). This explains why the $E_T$ remains constant from a carbazole dimer 2.75 eV to a carbazole trimer 2.74 eV. For the mixed carbazole/fluorene compounds, for example, carbazole-fluorene-carbazole linked via the 3,6 position of carbazole and the para position of fluorene (as illustrated in Figure 2b), the conjugation length extends to *p*-quaterphenyl by covering the inserted fluorene unit, and thus $E_T$ decreases to 2.38 eV.

The same behavior of variation of $E_T$ with chemical structure was held well in the poly(3,6-carbazole) derivatives.[4a,10b] Here, the triplet exciton of P(*t*Bu-CBP) can also be deduced from the above discussions and expected to be predominantly delocalized over the biphenyl unit across neighboring carbazole units as illustrated in Figure 2c. For P(*t*Bu-CBP*P*) and P(*t*Bu-CBP*F*), the triplet exciton can be expected to delocalize over the *p*-terphenyl and *p*-quaterphenyl units as illustrated in Figure 2c and b, respectively. Hence, an increased $\pi$-electron delocalization in these copolymers, P(*t*Bu-CBP*P*) and P(*t*Bu-CBP*F*), occurs as reflected in decreases of absorption and emission (especially for phosphorescence) energies as compared to P(*t*Bu-CBP). Consequently, to maintain high $E_T$ of conjugated polymer, the conjugation length of polymer should be carefully controlled. Dijken et al.[4a] found that, for maintaining high $E_T$ (2.56−2.6 eV), incorporation of a comonomer (e.g., oxadiazole or fluorene) into the carbazole main chain should only limit meta position coupling. Here, the high $E_T$ of the conjugated polymer is favorably obtained by the direct modification of a side group.

The HOMO levels of the present CBP-based polymers are close to each other; in other words, the copolymerization hardly affects the HOMO levels (Table 1). For P(*t*Bu-CBP), the side group acts as an inductive acceptor, leading to substantial lowering of the HOMO (as well as LUMO) with respect to P(3,6-Cz) by about 0.3 eV (0.2 eV). The reasons are as follows. First, for small molecules, an aryl substituent at the 9 position of carbazole was found to lower the HOMO level relative to the alkyl substituent, but only to a slight extent by about 0.1 eV.[10a] Second, the additional carbazole group attached on the side group of P(*t*Bu-CBP) can also enhance the inductive effect as in the case of tris(4-(9*H*-carbazol-9-yl)phenyl)amine (TCB), in which the incorporation of Cz on the three phenyl ring leads to a lowering in the HOMO and LUMO levels of triphenylamine (TPA) by 0.14 and 0.6 eV, respectively.[4b] This ensures the HOMO levels of CBP-based polymers are lower than or comparable to those of most reported Ir-complexes,[1c−d,2b,12] leading to the idea that Ir-complexes can act as a trap for hole carriers to promote efficient charge trapping.

**C. Absence of Excimer Emission in P(*t*Bu-CBP) Contrary to P(3,6-Cz).** Figure 3 shows UV−vis, PL, and PLE spectra of P(3,6-Cz) and P(*t*Bu-CBP) in solutions and as thin solid films. For P(3,6-Cz) thin solid film, the low-energy emission band (LEEB) centered at about 525 nm (Figures 1b and 3c) can be contributed from either an excimer or aggregates. An excimer is an emitting species that forms from a dimer of two molecules

(9) (a) Yang, X.; Neher, D.; Hertel, D.; Daubler, T. K. *Adv. Mater.* **2004**, *16*, 161−166. (b) Kawamura, Y.; Yanagida, S.; Forrest, S. R. *J. Appl. Phys.* **2002**, *92*, 87−93. (c) Lamansky, S.; Djurovich, P. I.; Abdel-Razzaq, F.; Garon, S.; Murphy, D. L.; Thompson, M. E. *J. Appl. Phys.* **2002**, *92*, 1570−1575.

(10) (a) Brunner, K.; Dijken, A. v.; Börner, H.; Bastiaansen, J. J. A. M.; Kiggen, N. M. M.; Langeveld B. M. W. *J. Am. Chem. Soc.* **2004**, *126*, 6035−6042. (b) Rothe, C.; Brunner, K.; Bach, I.; Heun, S.; Monkman, A. P. *J. Chem. Phys.* **2005**, *122*, 84706−1~84706−6.

(11) (a) Brike, J. B. *Photophysics of Aromatic Compounds*; John Wiley & Sons: New York, 1970. (b) Higuchi, J.; Hayashi, K.; Yagi, M.; Kondo, H. *J. Phys. Chem. A* **2002**, *106*, 8609−8618. (c) Higuchi, J.; Hayashi, K.; Seki, K.; Yagi, M.; Ishizu, K.; Kohno, M.; Ibuki, E.; Tajima, K. *J. Phys. Chem. A* **2001**, *105*, 6084−6091.

(12) (a) Lo, S. C.; Namdas, E. B.; Burn, P. L.; Samuel, I. D. W. *Macromolecules*, **2003**, *36*, 9721−9730. (b) Thomas, K. R. J.; Velusamy, M.; Lin, J. T.; Chien, C. H.; Tao, Y. T.; Wen, Y. S.; Hu, Y. H.; Chou, P. T. *Inorg. Chem.* **2005**, *44*, 5677−5685. (c) Sajoto, T.; Djurovich, P. I.; Tamayo, A.; Yousufuddin, M.; Bau, R.; Thompsom, M. E. *Inor. Chem.* **2005**, *44*, 7992−8003. (d) Huang, Y. T.; Chuang, T. H.; Shu, Y. L.; Kuo, Y. C.; Wu, P. L.; Yang, C. H.; Sun, I. W. *Organometallics* **2005**, *24*, 6230−6238. (e) Holmes. R. J.; Forrest, S. R.; Sajoto, T.; Tamayo, A.; Djurovich, P. I.; Thompsom, M. E.; Brooks, J.; Tung, Y. J.; D'Andrade, B. W.; Weaver, M. S. et al. *Appl. Phys. Lett.* **2005**, *87*, 243507−243507-3.

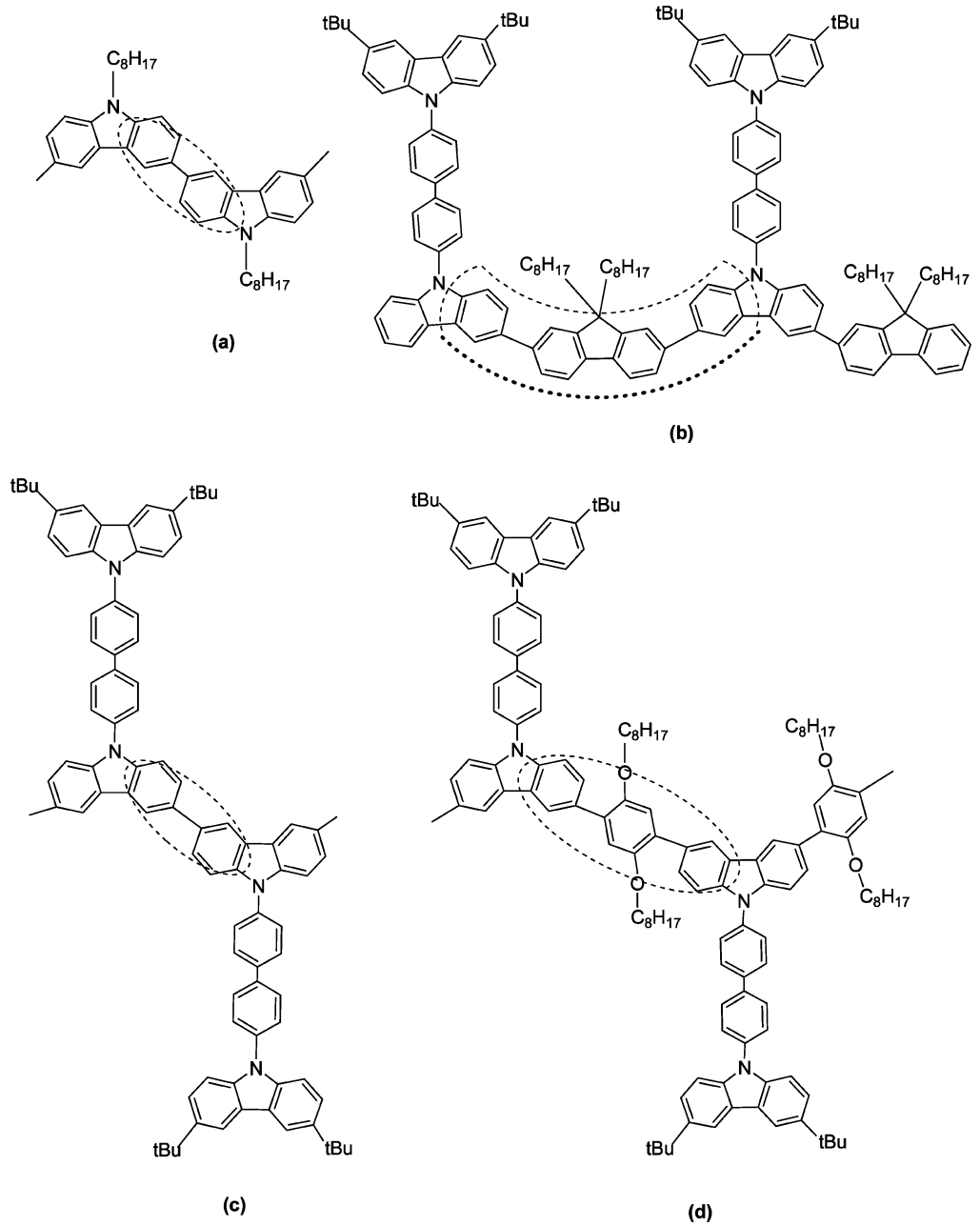


***Figure 2.*** Chemical structures of conjugated units in the four polymers investigated in this study. The dashed line indicated the presence of oligo(paraphenylene) in the polymer backbone.

of the same kind, one of which being in the excited state; it exists only at the excited state but is dissociative in the ground state. In contrast, an aggregate involves intermolecular interaction between two or more lumophores in the ground state by extending the delocalization of $\pi$-electrons over these conjugated segments. According to the method of characterization for aggregates in conjugated polymers used in our previous publications,[13] the LEEBs of P(3,6-Cz) are contributed from excimer rather than aggregates as to be revealed below.

For P(*t*Bu-CBP), the PL spectra of its solutions do not vary with concentration in the range $5 \times 10^{-4}$ to 5 mg/mL, and the PL spectrum of its spin-coated film is similar to that at the solution state except for a red shift in emission maximum ($\lambda_{max}$) by 3 nm (Figure 3b). Thus, there is no excimer or aggregate emitting species in P(*t*Bu-CBP) in solutions or as solid film. For P(3,6-Cz), the PL spectra of its solutions do not vary with concentration in the range $5 \times 10^{-4}$ to 5 mg/mL, but the PL spectrum of its spin-coated film shows a red shift in $\lambda_{max}$ by 6 nm and an additional LEEB centered at about 525 nm (Figure 3c). This indicates that new emission species (excimer or aggregates) form in P(3,6-Cz) thin solid film.

If the new emission species is aggregates, a new "red shift" and "structureless" aggregate emission should appear in the PL spectrum relative to the emission from the solutions at an excitation wavelength around the absorption edge, and a PLE spectrum monitored at the LEEB (500−650 nm here) should show a relatively elevated luminescence intensity in the longer wavelength region (>430 nm) over that monitored at 430 nm

(13) (a) Peng, K. Y.; Chen S. A.; Fann, W. S. *J. Am. Chem. Soc.* **2001**, *123*, 11388−11397. (b) Peng, K. Y.; Chen, S. A.; Fann, W. S.; Chen, S. H.; Su, A. C. *J. Phys. Chem. B* **2005**, *109*, 9368−9373.

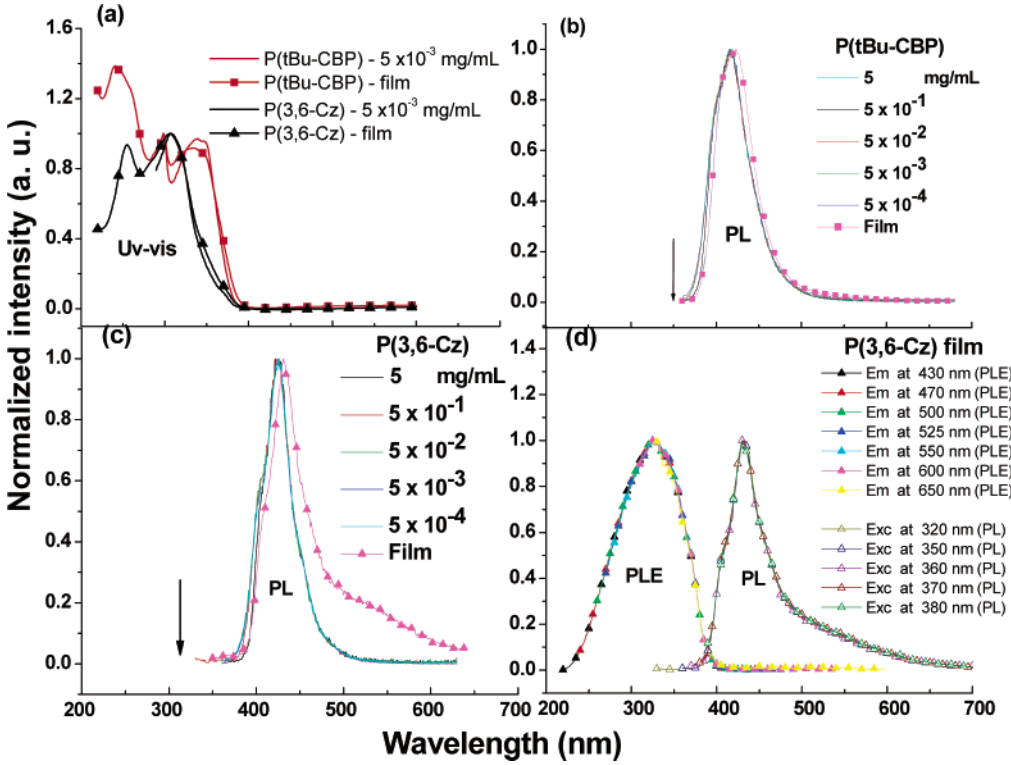


***Figure 3.*** (a) UV−vis spectra of P(3,6-Cz) and P(*t*Bu-CBP) solutions ($5 \times 10^{-3}$ mg/mL) in chlorobenzene and as thin solid film, (b) PL spectra of P(*t*Bu-CBP) solutions at various concentrations ($5 \times 10^{-4}$ to 5 mg/mL) and as thin solid film, (c) PL spectra of P(3,6-Cz) solutions at various concentrations ($5 \times 10^{-4}$ to 5 mg/mL) and as thin solid film, (d) PLE spectra of P(3,6-Cz) thin solid film monitored at various emission wavelengths (430−650 nm) and PL spectra of P(3,6-Cz) thin solid film excited at various excitation wavelengths (320−380 nm). The arrows in the PL spectra (b and c) indicate the excitation wavelength.

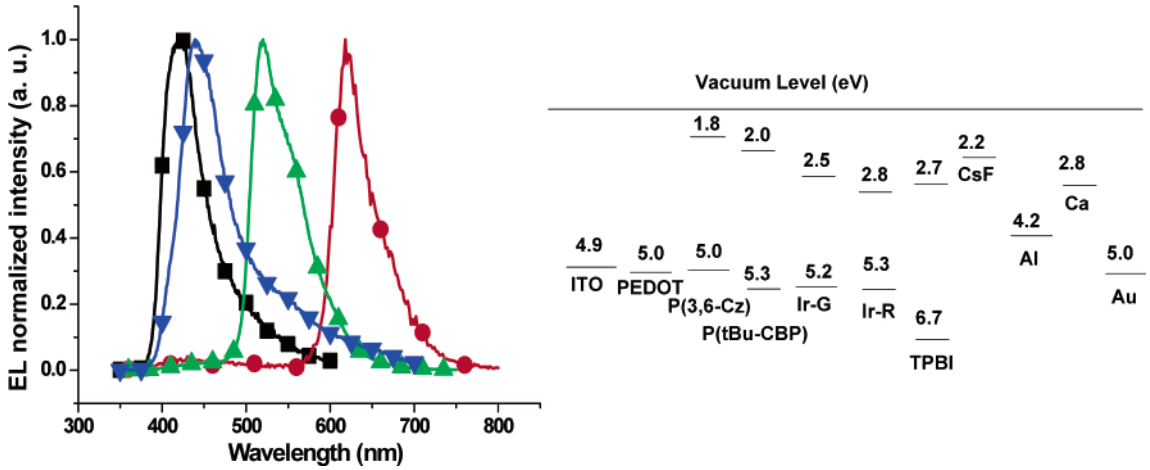


***Figure 4.*** Electroluminescence spectra of P(3,6-Cz) (▼) and P(*t*Bu-CBP) doped with Ir-complexes: 0 wt % dopant (■), 5 wt % Ir-R (●), and 8 wt % Ir-G (▲). The bipolar device structure is ITO/PEDOT:PSS (15 nm)/polymer or polymer:dopant (80 nm)/TPBI (30 nm)/CsF (2 nm)/Al. The band diagram is included on the right.

because of the existence of lumophore associates, which absorb light at longer wavelengths than the monomeric lumophores do.[13] However, no such aggregate emissions appear as also confirmed by the identical PLE spectra in P(3,6-Cz) thin solid film (Figure 3d). Thus the LEEBs are not from aggregates but from an excimer. Consequently, we can conclude that the LEEB in P(3,6-Cz) is an excimer emission and the side group of P(*t*Bu-CBP) can significantly suppress the formation of excimer.

**D. Green and Red Electrophosphorescence from the Device with P(*t*Bu-CBP) or P(3,6-Cz) as Host.** P(*t*Bu-CBP) has an $E_T$ (2.53 eV) higher than those of the green and red guests: bis(2-phenylpyridinato-*N*,$C^{2'}$)iridium(acetylacetonate) (denoted as Ir-G, $E_T = 2.41$ eV)[1c] and bis(1-phenyl-isoquinolinato-*N*,$C^{2'}$)iridium(acetylacetonate) (Ir−R, $E_T = 2.00$ eV);[14] it is therefore a potential host for both guests. Figure 4 shows electroluminescence spectra of P(3,6-Cz) and P(*t*Bu-CBP) doped with Ir-complexes and the band diagram of materials used in the bipolar device structure (ITO/PEDOT:PSS (15 nm)/polymer or doped polymer (80 nm)/TPBI (30 nm)/CsF (2 nm)/Al). The energy levels of Ir-G,[2b] Ir-R,[14] TPBI,[15a] and CsF[15b] are taken from the literatures. The work functions of ITO and PEDOT:PSS were measured by ultraviolet photoelectron spectroscopy

(14) Li, C. L.; Su, Y. J.; Tao, Y. T.; Chou, P. T.; Chien, C. H.; Cheng, C. C.; Liu, R. S. *Adv. Funct. Mater*. **2005**, *15*, 387−395.

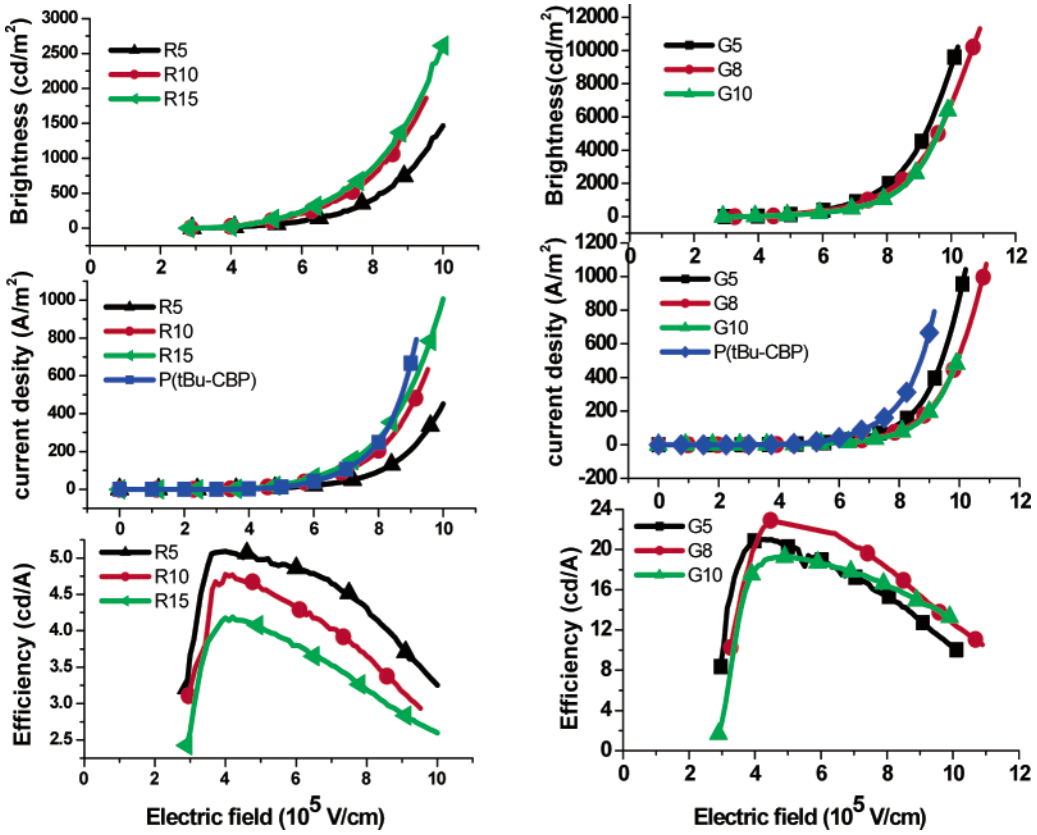


***Figure 5.*** Brightness (top), current density (middle), and efficiency (bottom) versus electric field for Ir-R doped devices (left) and for Ir-G doped devices (right). The Ir-R doping levels (by weight) are 5% (▲), 10% (●), and 15% (▼), and the Ir-G doping levels (by weight) are 5% (▲), 8% (●), and 15% (▼). Current density versus electric field for P(*t*Bu-CBP) (■) was put together with those for Ir-doped devices for a comparison. The unit for electric field ($10^5$ V/cm) is so taken so that, at the normal thickness of emitting layer 100 nm, the applied voltage is 1 V. The bipolar device structure is: ITO/PEDOT:PSS (15 nm)/P(*t*Bu-CBP) or doped P(*t*Bu-CBP) (80 nm)/TPBI (30 nm)/CsF (2 nm)/Al.

***Table 2.*** Device Performances of Ir-G or Ir-R as a Guest and P(*t*Bu-CBP), P(3,6-Cz), P(*t*Bu-CBPP), or P(*t*Bu-CBPF) as a Host[a]

| host | guest | turn-on (V) | $B_{max}$[b] (cd/m²) at cd/A | $\eta_{Lmax}$[b] (cd/A) at V | max $Q_{ext}$[b,c] (%) |
|---|---|---|---|---|---|
| P(*t*Bu-CBP) | 5 wt % Ir-R | 3.0 | 5590 (1.85) | 5.1 (4) | 4.23 |
| | 10 wt % Ir-R | 2.8 | 6910 (1.64) | 4.8 (4) | 3.98 |
| | 15 wt % Ir-R | 2.8 | 6450 (1.84) | 4.2 (4.2) | 3.48 |
| | 5 wt % Ir-G | 3.0 | 26 560 (5.11) | 21.0 (4.5) | 5.82 |
| | 8 wt % Ir-G | 2.9 | 31 500 (5.23) | 23.7 (4.3) | 6.57 |
| | 10 wt % Ir-G | 2.9 | 28 030 (5.95) | 19.3 (4.8) | 5.35 |
| P(3,6-Cz) | 5 wt % Ir-R | 2.9 | 980 (0.28) | 1.2 (4.1) | 1.0 |
| | 8 wt % Ir-G | 2.7 | 8160 (1.52) | 5.4 (4.3) | 1.5 |
| P(*t*Bu-CBP*P*) | 5 wt % Ir-R | 6.0 | 1800 (1.3) | 1.4 (15.7) | 1.17 |
| | 8 wt % Ir-G | 6.8 | 3400 (2.5) | 2.7 (16.9) | 0.75 |
| P(*t*Bu-CBP*F*) | 5 wt % Ir-R | 5.4 | 6750 (2.0) | 2.0 (17) | 1.67 |
| | 8 wt % Ir-G | 5.0 | 7800 (2.3) | 2.6 (13.7) | 0.72 |

[a] The device structure is ITO/PEDOT:PSS (15 nm)/Polymer:dopant (80 nm)/TPBI (30 nm)/CsF (2 nm)/Al. (*t*Bu-CBP) and P(3,6-Cz) were dissolved in chlorobenzene (20 mg/mL) and P(*t*Bu-CBP*P*) and P(*t*Bu-CBP*F*) in tetrahydrofuran (10 mg/mL). [b] The data for brightness ($B_{max}$), luminous efficiency ($\eta_{Lmax}$), and external quantum efficiency ($Q_{ext}$) are the maximum values of the device. The turn-on voltage was taken at 0.2 cd/m². [c] $Q_{ext}$ was calculated from the total photon number evaluated from luminance and emission spectra on the assumption that the spatial emission pattern from the PLEDs was Lambertian.

(UPS). The emission spectrum of P(*t*Bu-CBP) has a peak at 420 nm and no lower-energy emission (which appears in P(3,6-Cz)s and was claimed from an electromer),[4a] indicating that the bulky side group of *t*Bu-CBP can suppress the stacking of carbazole units in the main chain. Complete emissions from Ir-G (519 nm) and Ir-R (618 nm) are observed in the devices with the dopants above 5 wt % and identical to the PL spectra of the dopants, respectively.

Table 2 lists the performances (brightness, turn-on voltage, luminous and external quantum efficiencies) of the devices with the Ir-complexes doped with polymers at various doping levels, and Figure 5 shows the brightness, current density, and efficiency versus electric field for Ir-R and Ir-G doped P(*t*Bu-CBP) devices. For P(*t*Bu-CBP), the best device performances for Ir-R ($\eta_{Lmax}$ = 5.1 cd/A, corresponding $Q_{ext}$ = 4.23%; $B_{max}$ = 5590 cd/m²) and Ir-G ($\eta_{Lmax}$ = 23.7 cd/A, corresponding $Q_{ext}$ = 6.57%; $B_{max}$ = 31 500 cd/m²) are observed at the optimal doping levels 5 and 8 wt %, respectively, both exhibiting low turn-on voltage (~3 V) (Table 2 and Figure 5). The present green emission device is as efficient as that with the reported carbazole copolymer doped by an Ir-G with dendrimer-like ligands[16a] (the most efficient green emission device with a conjugated polymer, $\eta_{Lmax}$ = 23 cd/A),[4a] even though the present Ir-G seems to have a higher tendency toward phase separation, as evidenced in Figure 6, than this Ir-G ligand, and might lead to an inefficient use of guest molecules and a promoted triplet−triplet annihilation.[16] Figure 6 shows the SPM phase-contrast images of both polymers, P(*t*Bu-CBP) and P(3,6-Cz), doped with the Ir-complexes and of their pristine polymer films. We find that phase separation occurs in the Ir-complexes doped polymers, as shown in Figure 6b, c, e, and f. But the extent of

(15) (a) Anthopoulos, T. D.; Markham, J. P. J.; Namdas, E. B.; Samuel, I. D. W.; Lo, S. C.; Burn, P. L. *Appl. Phys. Lett.* **2003**, *82*, 4842−4826. (b) Michaelson, H. B. *J. Appl. Phys.* **1977**, *48*, 4729−4733.

(16) (a) Lo, S.-C.; Male, N. A. H.; Markham, J. P. J.; Magennis, S. W.; Burn, P. L.; Salata, O. V.; Samuel, I. D. W. *Adv. Mater.* **2002**, *14*, 975−979. (b) Yang, X.; Neher, D.; Hertel, D.; Däubler, T. K. *Adv. Mater.* **2004**, *16*, 161−166.

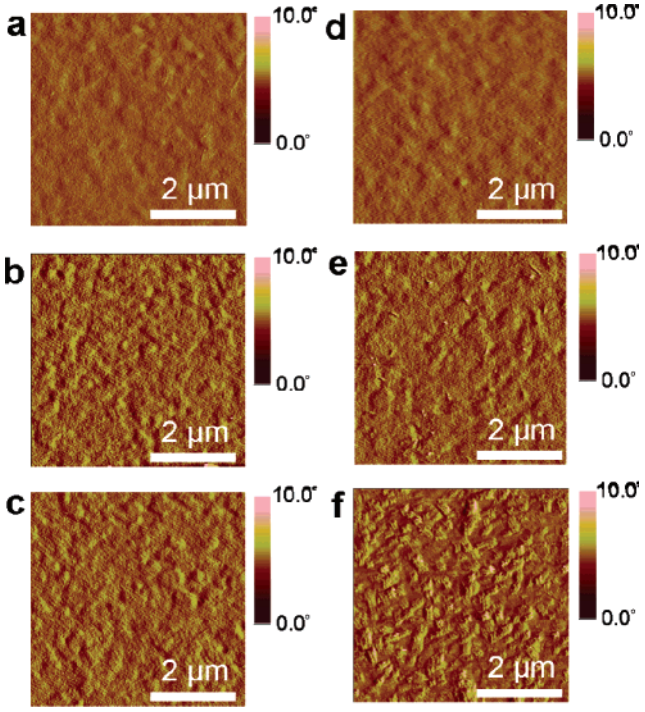


***Figure 6.*** Phase-contrast image of the six polymer samples, (a) P(*t*Bu-CBP), (b) P(*t*Bu-CBP) doped with 8 wt % Ir-G, (c) P(*t*Bu-CBP) doped with 5 wt % Ir-R, (d) P(3,6-Cz), (e) P(3,6-Cz) doped with 8 wt % Ir-G, and (f) P(3,6-Cz) doped with 5 wt % Ir-R, as measured using a scanning probe microscope (from Digital Instrument Nanoscope III).

phase separation for the case with P(*t*Bu-CBP) is less than that with P(3,6-Cz). Consequently, the doped devices show fast decay in efficiency with the electric field as shown in Figures 5 and 7.

For the polymer with the same backbone, P(3,6-Cz), at the above optimal Ir-R and Ir-G doping levels for P(*t*Bu-CBP), the corresponding $B_{max}$ and $\eta_{Lmax}$ are both lower by a factor of 4 (Table 2 and Figures 6), even though it has an $E_T$ higher than that of P(*t*Bu-CBP) by 0.07 eV. Thus the higher efficiency in doped P(*t*Bu-CBP) devices is not only due to its high $E_T$ but also its side group which may also play some role. As the two copolymers P(*t*Bu-CBP*P*) and P(*t*Bu-CBP*F*) are used as hosts, the devices with the dopants Ir−R and Ir-G at the doping levels 5 and 8 wt % give an efficiency lower by factors of about 3 (R) and 9 (G) relative to those with P(*t*Bu-CBP) as the host (Table 2), even though the HOMO and LUMO levels of the three polymers are close (Table 1). Thus, such lowering in efficiency must be due to an increased back transfer of triplet energy from the dopant to the host.

**E. Why P(*t*Bu-CBP) Performs Better Than P(3,6-Cz)?** To understand why P(*t*Bu-CBP) is a good host for an efficient device, the charge transport properties of P(*t*Bu-CBP) and P(3,6-Cz) are investigated by single-carrier devices,[17] and the results are shown in Figure 8. P(*t*Bu-CBP) shows balanced electron and hole fluxes, while P(3,6-Cz) shows the current density of the hole is higher than that of the electron by 2 orders of magnitude at 4 × $10^5$ V/cm. The results can be explained by

(17) (a) Blom, P. W. M.; de Jong, M. J. M.; Vleggaar, J. J. M. *Appl. Phys. Lett.* **1996**, *68*, 3308−3310. (b) Yu, L. S.; Tseng, H. E.; Lu, H. H.; Chen, S. A. *Appl. Phys. Lett.* **2002**, *81*, 2014−2016. (c) Yu, L. S.; Chen, S. A. *Adv. Mater.* **2004**, *16*, 744−748. (d) Hsiao, C. C.; Chang, C. H.; Jen, T. H.; Hung, M. C.; Chen, S. A. *Appl. Phys. Lett.* **2006**, *88*, 33512−33512-3.

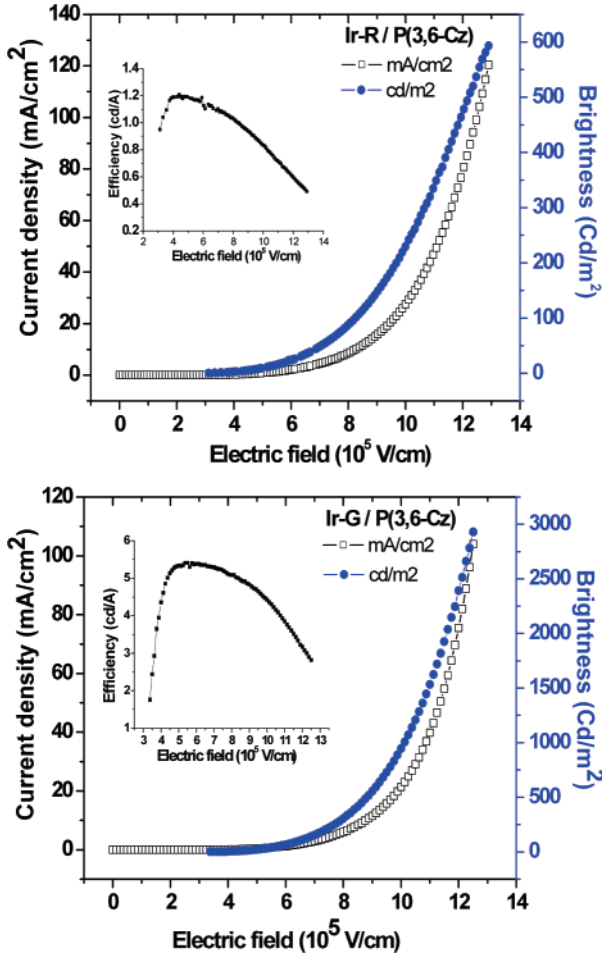


***Figure 7.*** Brightness (●) and current density (□) versus electric field for 5 wt % Ir-R doped devices (left) and for 8 wt % Ir-G doped devices (right). The inset is the efficiency versus electric field. The unit for electric field ($10^5$ V/cm) is so taken so that, at the normal thickness of emitting layer 100 nm, the applied voltage is 1 V. The bipolar device structure is: ITO/PEDOT:PSS (15 nm)/doped P(3,6-Cz) (80 nm)/TPBI (30 nm)/CsF (2 nm)/Al.

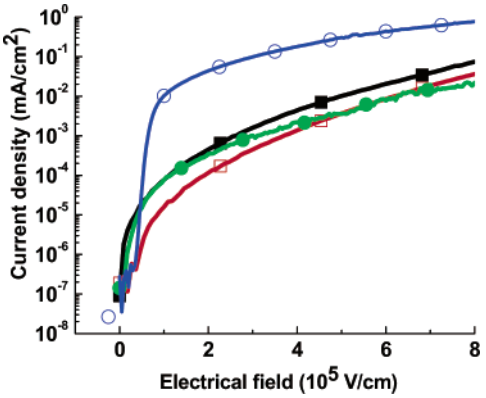


***Figure 8.*** Current density versus electric field for single carrier devices with P(3,6-Cz) (○ for hole and ● for electron) and P(*t*Bu-CBP) (□ for hole and ■ for electron) as the active polymer layer. The hole and electron dominating device structures are ITO/PEDOT:PSS/Polymer/Au and ITO/Ca/Polymer/CsF/Al, respectively.

the HOMO and LUMO energy levels of both polymers (Figure 4). For P(*t*Bu-CBP), the injection barrier for the hole (0.3 eV) is close to that for the electron (0.2 eV) (referred to as the anode PEDOT:PSS and the cathode CsF/Al), whereas, for P(3,6-Cz),

the injection barrier for the hole (0 eV) is much smaller than that for the electron (0.4 eV).

In addition, both Ir-G and Ir-R can act as traps for both electron and hole carriers in P(*t*Bu-CBP) as a host, but for P(3,6-Cz), it only acts as an electron trap based on their corresponding HOMO and LUMO levels (Figure 4). The other factor that leads to the improvement could be due to the enhancement of PLQE, which results in a more efficient Förster energy transfer from the host to the guest.[6,18]

## Conclusions and Significance

In conclusion, we found that the high $E_T$ of conjugated polymer P(*t*Bu-CBP) exhibits balanced charge flux characteristics. Upon doping with Ir-R and Ir-G, devices with high efficiency and brightness for green and red emissions can be obtained which are higher than the case with the polymer having the same backbone and higher $E_T$, P(3,6-Cz), as the host. The results reflect that, in the phosphorescent device, the difference in $E_T$ between the host and guest is not the only factor that determines the device efficiency, and the present side group modification via the 9 position of carbazole also plays an important role, which allows a tuning of HOMO and LUMO levels for balancing electron and hole fluxes and provides a depression of formation of excimer. Also, the tuning of HOMO/LUMO levels allows a charge trapping of both electron and hole in the dopants to occur. Thus, the present work provides a new route for designing ambipolar transporting polymers with energy level matching and high $E_T$, simultaneously.

**Acknowledgment.** We thank the MOE for financial aid through Project 91E-FA04-2-4A, the NSC for constant financial support in the past, and Dr. Xiwen Chen for fruitful discussions.

**Supporting Information Available:** Instrumentation details, detailed experimental procedures, and characterizations for all the monomers and polymers. This material is available free of charge via the Internet at http://pubs.acs.org.

JA060936T

(18) Shoustikov, A.; You, Y.; Burrows, P. E.; Thompson, M. E.; Forrest, S. R. *Synth. Met.* **1997**, *91*, 217−221.